

# TCF7L2 Regulates Late Events in Insulin Secretion From Pancreatic Islet $\beta$ -Cells

Gabriela da Silva Xavier,<sup>1</sup> Merewyn K. Loder,<sup>1</sup> Angela McDonald,<sup>1</sup> Andrei I. Tarasov,<sup>1</sup> Raffaella Carzaniga,<sup>2</sup> Katrin Kronenberger,<sup>2</sup> Sebastian Barg,<sup>3</sup> and Guy A. Rutter<sup>1</sup>

**OBJECTIVE**—Polymorphisms in the human *TCF7L2* gene are associated with reduced insulin secretion and an increased risk of type 2 diabetes. However, the mechanisms by which *TCF7L2* affect insulin secretion are still unclear. We define the effects of *TCF7L2* expression level on mature  $\beta$ -cell function and suggest a potential mechanism for its actions.

**RESEARCH DESIGN AND METHODS**—*TCF7L2* expression in rodent islets and  $\beta$ -cell lines was altered using RNAi or adenoviral transduction.  $\beta$ -Cell gene profiles were measured by quantitative real-time PCR and the effects on intracellular signaling and exocytosis by live cell imaging, electron microscopy, and patch clamp electrophysiology.

**RESULTS**—Reducing *TCF7L2* expression levels by RNAi decreased glucose- but not KCl-induced insulin secretion. The glucose-induced increments in both ATP/ADP ratio and cytosolic free  $\text{Ca}^{2+}$  concentration ( $[\text{Ca}^{2+}]_i$ ) were increased compared with controls. Overexpression of *TCF7L2* exerted minor inhibitory effects on glucose-regulated changes in  $[\text{Ca}^{2+}]_i$  and insulin release. Gene expression profiling in *TCF7L2*-silenced cells revealed increased levels of mRNA encoding syntaxin 1A but decreased *Munc18-1* and *ZnT8* mRNA. Whereas the number of morphologically docked vesicles was unchanged by *TCF7L2* suppression, secretory granule movement increased and capacitance changes decreased, indicative of defective vesicle fusion.

**CONCLUSION**—*TCF7L2* is involved in maintaining expression of  $\beta$ -cell genes regulating secretory granule fusion. Defective insulin exocytosis may thus underlie increased diabetes incidence in carriers of the at-risk *TCF7L2* alleles. *Diabetes* 58: 894–905, 2009

**T**ype 2 diabetes is the most common metabolic disease in industrialized societies (1). The disease has a complex etiology involving interplay between environmental risk factors (obesogenic diet, lack of exercise) and a susceptible genetic background (2). Although the hereditary nature of type 2 diabetes has been acknowledged for many years (3), only recently have candidate gene studies (4–6) and whole

genome association approaches (7–10) identified polymorphisms in 12 specific gene loci that increase disease risk. These, and an earlier candidate gene study (11), identified single nucleotide polymorphisms (SNPs), including SNP rs7903146, in the third intron of the gene encoding transcription factor 7-like 2 (*TCF7L2*; also known as transcription factor 4) as strongly associated with type 2 diabetes in different ethnic backgrounds (9–13). rs7903146 has been estimated to contribute to 10 to 25% of all cases of diabetes in lean individuals (14).

*TCF7L2* is a member of the T-cell-specific high-mobility group box-containing family of transcription factors that, on binding  $\beta$ -catenin, transduces signals generated by *Wnt* receptors at the cell surface to modify expression of multiple genes, many of which are associated with the cell cycle (15). Mutations in *TCF7L2* are also implicated in certain types of cancer (16).

Recent clinical studies have demonstrated that the at-risk SNP is associated with maintained insulin sensitivity (HOMA-B) but defects in  $\beta$ -cell function and insulin release (17). Because the SNP is found in an intronic region, a potential mechanism through which it may confer an increased risk of diabetes is by altering *TCF7L2* expression levels. A recent study by Lyssenko and colleagues (18) suggested that pancreatic islets from patients with type 2 diabetes bearing the at-risk TT allele have increased *TCF7L2* RNA levels, indicating that excessive *TCF7L2* expression may be associated with the reported insulin-secretory defects. Expression studies carried out by Elbein and colleagues (19) on adipose tissue and muscle showed that *TCF7L2* expression was not altered by genotype and did not correlate with insulin sensitivity or BMI. *TCF7L2* mRNA levels in subcutaneous white adipose tissue from TT-bearing individuals were decreased compared with those in control (CC-bearing) individuals (20,21). At present, data on *TCF7L2* expression levels in individuals carrying the at-risk allele are inconclusive, and given the possibility of alternate splicing, it remains to be established how the level of active *TCF7L2* is altered.

Homozygous *pcf7l2* knockout mice die shortly after birth with profound changes in gut development involving failed conversion of the endoderm to epithelial progenitors (22). Although detailed morphometric analyses have yet to be reported, pancreatic development is grossly normal in homozygous mutant mice (22). A recent study in isolated human islets demonstrated that RNAi-mediated depletion of *TCF7L2* mRNA led to ablation of glucose-stimulated insulin secretion and increased  $\beta$ -cell apoptosis (23). To date, the mechanisms through which functional *TCF7L2* modulates glucose sensing and insulin release in pancreatic  $\beta$ -cells are unknown.

We provide a detailed investigation of the effects of altering *TCF7L2* content on  $\beta$ -cell function and on the expression of genes pivotal to  $\beta$ -cell glucose sensing. We

From the <sup>1</sup>Section of Cell Biology, Division of Medicine, Faculty of Medicine, Imperial College, London, U.K.; the <sup>2</sup>Electron Microscopy Centre, Imperial College London, South Kensington, U.K.; and <sup>3</sup>Medical Cell Biology, Uppsala University, Uppsala, Sweden.

Corresponding author: Guy A. Rutter, g.rutter@imperial.ac.uk.

Received 29 August 2008 and accepted 14 January 2009.

Published ahead of print at <http://diabetes.diabetesjournals.org> on 23 January 2009. DOI: 10.2337/db08-1187.

G.d.S.X., M.K.L., and A.M. contributed equally to this work.

© 2009 by the American Diabetes Association. Readers may use this article as long as the work is properly cited, the use is educational and not for profit, and the work is not altered. See <http://creativecommons.org/licenses/by-nc-nd/3.0/> for details.

The costs of publication of this article were defrayed in part by the payment of page charges. This article must therefore be hereby marked "advertisement" in accordance with 18 U.S.C. Section 1734 solely to indicate this fact.

See accompanying commentary, p. 800.

show that silencing of TCF7L2 in primary mouse islets as well as in clonal MIN6 and INS-1(832/13) cells decreases both basal- and glucose-stimulated insulin secretion. TCF7L2 silencing also abolished the stimulatory effects of GLP-1 on secretion while having little impact on glucose-induced changes in intracellular ATP or free  $\text{Ca}^{2+}$  concentrations. We also show that TCF7L2 controls the expression of genes involved in insulin granule fusion at the plasma membrane. These changes may underlie defective insulin secretion in  $\beta$ -cells lacking TCF7L2.

## RESEARCH DESIGN AND METHODS

All reagents were purchased from Sigma (Poole, U.K.) or GIBCO-BRL (Paisley, U.K.) unless otherwise stated. Mouse monoclonal antibody for TCF7L2 was purchased from Abnova (Taiwan).

**Culture of MIN6 and INS-1(832/13)  $\beta$ -cell lines.** MIN6  $\beta$ -cells were used between passages 19 and 30 and cultured as previously described (24). INS-1(832/13) cells were cultured as described (25). Cells were transfected with plasmids and siRNA using Lipofectamine 2000 (Invitrogen, Paisley, U.K.) or TransIT-TKO (Mirus Bio Corporation, Madison, WI), respectively, according to the manufacturer's instructions.

**Isolation and culture of mouse islets.** Islets were isolated from female CD1 mice and cultured as described (26).

**TCF7L2 silencing.** siRNA against mouse and rat TCF7L2 (sense-AAGAAGC-CCCTTAATGCATTCTGTCTC, antisense-AATGCATTAAGGGGCTTCCTTC-CTGTCTC) and control siRNA (sense-AACCCGCAATTTAGAAGCATT-CCTGTCTC, antisense-AATGCTTCTAAATTGCGGGTTCCTGTCTC) were designed according to criteria set out by Tuschl and associates (<http://www.rockefeller.edu/labheads/tuschl/sirna.html> and references therein) and synthesized using Ambion's Silencer siRNA kit (Ambion, Austin, TX). Fluorescein-labeled siRNA duplexes of these sequences were from Sigma Genosys. Enhanced green fluorescent protein (EGFP)-tagged shRNA, based on the previously mentioned siRNA, was synthesized by annealing oligonucleotides containing the sequences for scrambled or TCF7L2 shRNA into pcDNA6.2/GW/mir-EGFP (Invitrogen).

**Overexpression of TCF7L2 in rodent  $\beta$ -cells.** Human TCF7L2 cDNA (OriGene Technologies) was cloned into pEGFP-N1. TCF7L2-EGFP adenovirus was generated as previously described (<http://www.coloncancer.org/adeasy.htm>). Cells were infected with control or TCF7L2-EGFP adenovirus at 100 MOI for 48 h before experiments.

**Real-time PCR analysis.** Primers for real-time PCR analysis were designed using Primer Express 3.0 (Applied Biosystems, Foster City, CA) using mRNA sequences for mouse and rat on the Ensembl database (<http://www.ensembl.org/>). Sequence specificity for all primers was verified using BLAST (<http://www.ncbi.nlm.nih.gov/blast/>). Real time-PCR was performed on an ABI-Prism Fast 7500 device (Applied Biosystems) using powerSYBR reagent (Applied Biosystems).

**Insulin secretion.** Mouse islets and clonal cell lines were cultured in the presence of siRNA (1 nmol/l or 10 nmol/l, respectively) for 48 h before insulin secretion assay in Krebs-Ringer Bicarbonate Buffer (KRB; 125 mmol/l NaCl, 3.5 mmol/l KCl, 1.5 mmol/l  $\text{CaCl}_2$ , 0.5 mmol/l  $\text{NaH}_2\text{PO}_4$ , 0.5 mmol/l  $\text{MgSO}_4$ , 3 mmol/l glucose, 10 mmol/l HEPES, and 2 mmol/l  $\text{NaHCO}_3$ , pH 7.4, and equilibrated with  $\text{O}_2/\text{CO}_2$  [95:5] and supplemented with 0.1% [wt/vol] BSA) (26,27). Secreted insulin was measured by radioimmunoassay (LINCO/Millipore, St. Charles, MO).

**Intracellular  $[\text{Ca}^{2+}]$  imaging.** INS-1(832/13) cells or mouse islets were transfected 48 h before assay. INS-1(832/13) cells (incubated overnight in media containing 3 mmol/l glucose) or dispersed islets were incubated for 30 min in KRB containing 3 mmol/l glucose and 200 nmol/l FURA-RED AM (Invitrogen). Cells were stimulated using the conditions indicated and excited at 480/440 nm using an Olympus IX-81 microscope coupled to an F-view camera and captured using CellR software (Olympus, Hertfordshire, U.K.) with a 40 $\times$  oil objective. Data were expressed as the ratio of the fluorescence emission at 440/480 nm. The AUC was calculated using OriginPro7.5 software (OriginLab, Northampton, MA) and statistical tests by ANOVA using GraphPad Prism 4.0 (GraphPad Software).

**Dual-color total internal reflection fluorescence (TIRF) microscopy.** Transfected MIN6 cells were imaged at 30°C in KRB with 3 mmol/l glucose using a custom-built lens-type TIRF microscope based on an inverted stand (Axiovert 200M; Carl Zeiss) and equipped with a 100 $\times$ /1.45 Apo lens (Carl Zeiss). Cells were excited using DPSS lasers (473 nm, 80 mW [EGFP] and 555 nm, 25 mW [mCherry]; Crystalasers) Emitted light was separated using a double dichroic (59022 bs) magnified with an Optovar 1.6 (Carl Zeiss) and split into two channels using an image splitter (DualView; Optical Insights, Santa

Fe, NM) with a dichroic cutoff at 585 nm (T585LP) and bandpass filters 595 to 670 nm (ET630-75) and 485 to 550 nm (ET517/65M). All filters were from Chroma. Separate images of the two channels were taken on a CCD camera (Cascade 512B; Roper Scientific, Trenton, NJ, or iXon<sup>EM</sup> + DU-897; Andor Technology, Belfast, U.K.).

Cells were selected based on green fluorescence and morphology. Granules were detected automatically with an in-house algorithm written as a MetaMorph journal. The image was subjected to morphological tophat, H-Dome, and dilate operations before internal thresholding and counting of objects. A threshold was set by the operator once for the entire dataset.

**Granule dynamics.** All granule tracks were selected for each time period using an Image J software particle tracker. The movement of each granule between frames was then analyzed according to the equation  $\sqrt{[(x_2 - x_1)^2] + [y_2 - y_1]^2}$  [2] and converted to microns per second generating a range of granule movement velocities. The results were expressed as the number of movements occurring at each velocity. Two distinct subgroups of granules were observed (fixed and moving), and analysis of the percentage of granules in each subgroup was determined by curve fitting to two sites (Origin Software).

**Confocal microscopy.** Paraformaldehyde (4% wt/vol) fixed INS-1(832/13) cells previously transfected with either pEGFP-N1 or TCF7L2-pEGFP-N1 were imaged using a Zeiss Axiovert 200M microscope fitted with a PlanApo  $\times$ 63 oil-immersion objective and a 1.5 $\times$  optivar. Sample illumination at 345 and 492 nm and data acquisition were controlled with an Improvison/Noldigawa spinning disc system running Velocity (Improvison, Coventry, U.K.) software. **Total adenine nucleotide measurements.** ATP (28) and ADP (29) were quantified as previously described.

**Electron microscopy.** Isolated islets were treated with siRNA and glucose as for secretion assays described previously and then fixed in formaldehyde-glutaraldehyde for 30 min at 37°C and postfixed in 1.0% osmium tetroxide. Samples were processed for embedding in epon. Serial ultrathin 80-nm sections were poststained with saturated methanolic uranyl acetate and Reynold's lead citrate and observed with a transmission electron microscope (Tecnai G2 Spirit-FEI Company) at an operating voltage of 120 kV. Images were collected using TEM v3.1 software (FEI Company) at a magnification of  $\times$ 2,700 with a 2k  $\times$  2k CCD camera (Eagle; FEI Company). Islets were sectioned at 20  $\mu$ m and 40  $\mu$ m from the surface and four cells imaged per section. All imaging was carried out blind to treatment condition.

**Analysis of electron microscopy images.** Morphologically docked granules were defined using criteria previously described (30). To control for variations in cell size resulting from the plane of section, the length of plasma membrane was measured and the data expressed as granules per micron. Total granule content was defined as the granule number per micron squared of cytosol. Statistical analysis was by ANOVA with Bonferroni post hoc analysis.

**Electrophysiology.** Electrical capacitance ( $C_m$ ) and  $\text{Ca}^{2+}$  current ( $I_{\text{Ca}}$ ) through the plasma membrane of  $\beta$ -cells were recorded using a EPC9 patch-clamp amplifier controlled by Pulse software (HEKA Elektronik, Lambrecht/Pfalz, Germany) in standard whole-cell configuration. Single  $\beta$ -cells from dispersed mouse islets were transfected with fluorescein-labeled siRNA as described for  $\text{Ca}^{2+}$  imaging.

Cells were voltage-clamped at  $-70$  mV, and exocytosis was elicited by trains of 200, 500, or 2,500 ms depolarizations to 10 mV essentially as previously described (31). Noise reduction (1-D quadratic Loess) and data analysis were performed using IgorPro software (Wavemetrics, Lake Oswego, OR).

Data are given as means  $\pm$  SE of three to six individual experiments. Unless otherwise described, comparisons between means were performed using Student's *t* test with Microsoft Excel.

## RESULTS

**Impact of TCF7L2 silencing on regulated insulin secretion.** The presence of TCF7L2 mRNA and protein was confirmed in mouse islets, MIN6 (mouse) and INS-1(832/13) (rat) clonal  $\beta$ -cells (Fig. 1A–C, respectively) consistent with the reported expression of this protein in human islets (18,23). Endogenous TCF7L2 mRNA levels did not change in response to changing glucose concentrations in MIN6 and INS-1(832/13) cells (Fig. 1B and C). Of three siRNAs designed against TCF7L2, one provided substantial knockdown ( $76 \pm 0.2\%$ ,  $n = 3$  versus scrambled siRNA-treated cells) in TCF7L2 immunoreactivity in mouse islets (Fig. 1A) after 48 h of siRNA treatment and near total ablation of TCF7L2 immunoreactivity in MIN6 (Fig. 1B) and INS-1(832/13) (Fig. 1C)  $\beta$ -cells.



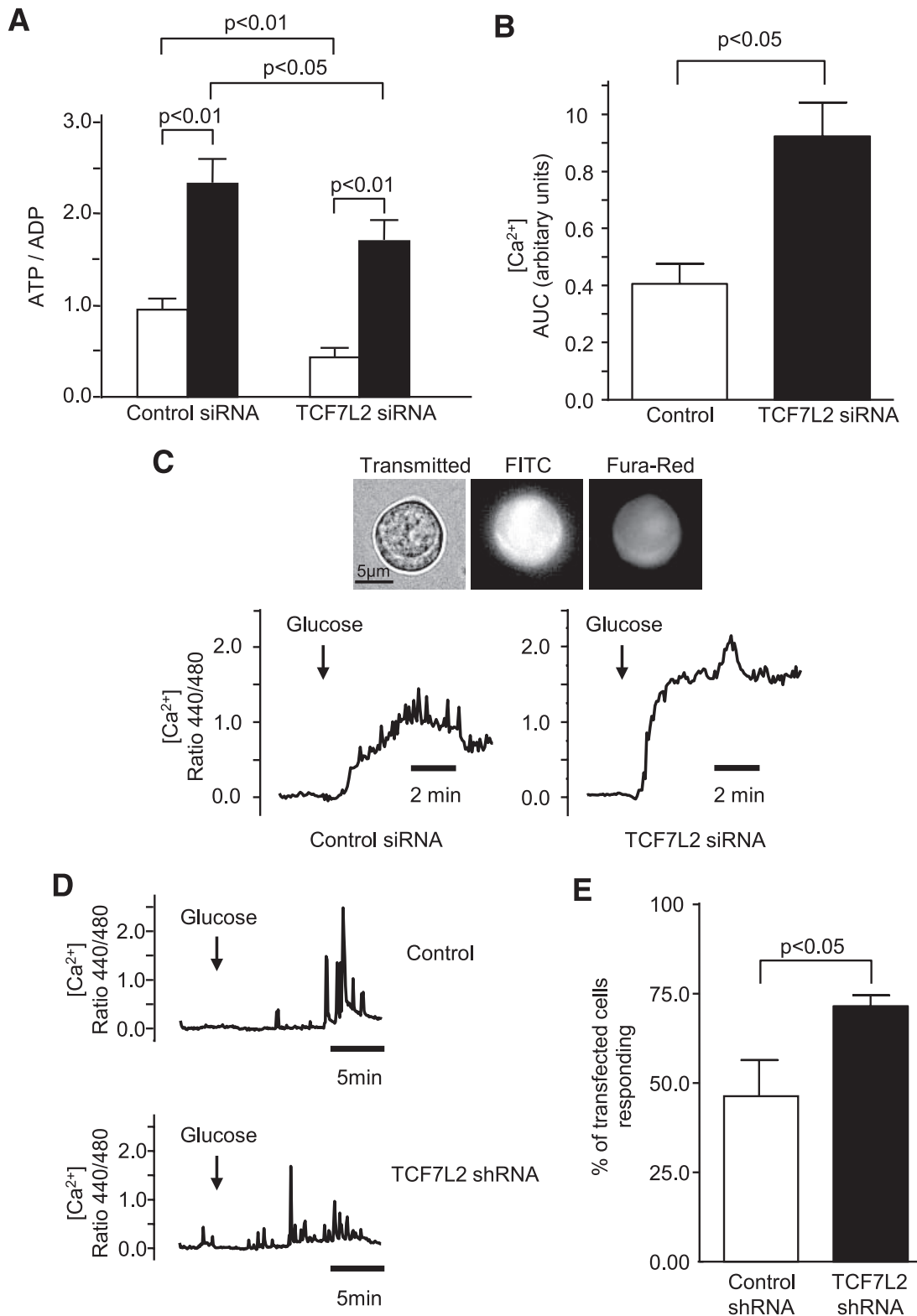


**FIG. 2.** TCF7L2 knockdown in mouse pancreatic islets and INS-1(832/13)  $\beta$ -cells does not alter glucose-stimulated changes in intracellular free  $[Ca^{2+}]$  but alters total cellular ATP and ADP levels. Mouse islets were treated and intracellular adenine nucleotide measured as described in RESEARCH DESIGN AND METHODS (A). Dissociated mouse islet cells (B and C) and INS-1(832/13)  $\beta$ -cells (D and E) were treated with 10 nmol/l fluorescein-labeled siRNA (B and C) or pEGFP-TCF7L2 shRNA (D and E) and incubated with FURA-Red (200 nmol/l; B–E) for  $[Ca^{2+}]$  measurement. Typical traces are shown (C and D). Glucose-induced (3.0 versus 11 mmol/l)  $[Ca^{2+}]$  changes in individual glucose-responsive dissociated mouse islet cells in which TCF7L2 was silenced (B) and the number of INS-1(832/13) cells within the cell population that responded to (20 mmol/l) glucose (E) are shown. Data are means  $\pm$  SEM,  $n = 3$ , unless otherwise stated in the RESEARCH DESIGN AND METHODS. AUC, area under the curve; FITC, fluorescein isothiocyanate.

Silencing of TCF7L2 in mouse islets had no significant effect on total islet insulin content ( $74.9 \pm 4.4$  versus  $69.7 \pm 3.2$  ng/islet,  $n = 3$ ; 54 islets per condition), but

resulted in a decrease in both the basal (3 mmol/l) and glucose stimulated (11 mmol/l) insulin release (Fig. 1A). Similar changes were seen in two  $\beta$ -cell lines (Fig. 1B and

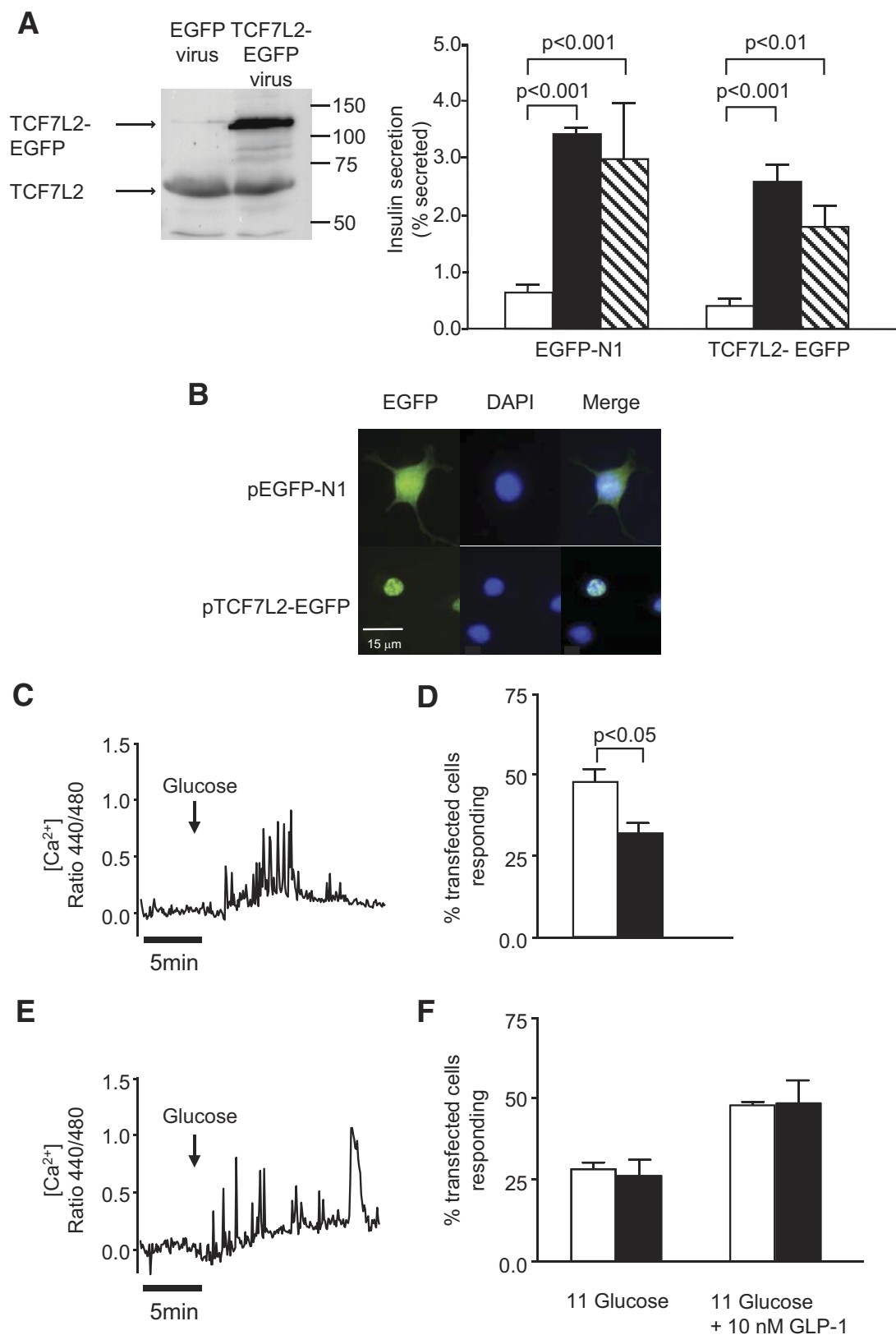


**FIG. 3. A:** Overexpression of TCF7L2-EGFP has no effect on glucose-stimulated insulin secretion. Insulin secretion from mouse islets overexpressing TCF7L2-EGFP was assessed as described in RESEARCH DESIGN AND METHODS. □, 3.0 mmol/l glucose; ■, 15 mmol/l glucose; ▨, 3.0 mmol/l glucose + KCl. **B:** Overexpression and subcellular localization of TCF7L2-EGFP in INS-1(832/13) cells was assessed by confocal microscopy 48 h after plasmid transfection. Scale bar = 15  $\mu$ m. [Ca<sup>2+</sup>]<sub>i</sub> imaging was performed as described in RESEARCH DESIGN AND METHODS. **C and E:** Representative traces of [Ca<sup>2+</sup>]<sub>i</sub> responses to glucose (3 versus 20 mmol/l) stimulation are shown for EGFP-N1 vector (**C**) and TCF7L2-EGFP (**E**). The proportion of cells that displayed glucose- or GLP-1-induced [Ca<sup>2+</sup>]<sub>i</sub> changes are shown in **D** and **F**, respectively (□, EGFP-N1; ■, TCF7L2-EGFP). Data are means  $\pm$  SEM,  $n = 3$ . (A high-quality digital representation of this figure is available in the online issue.)

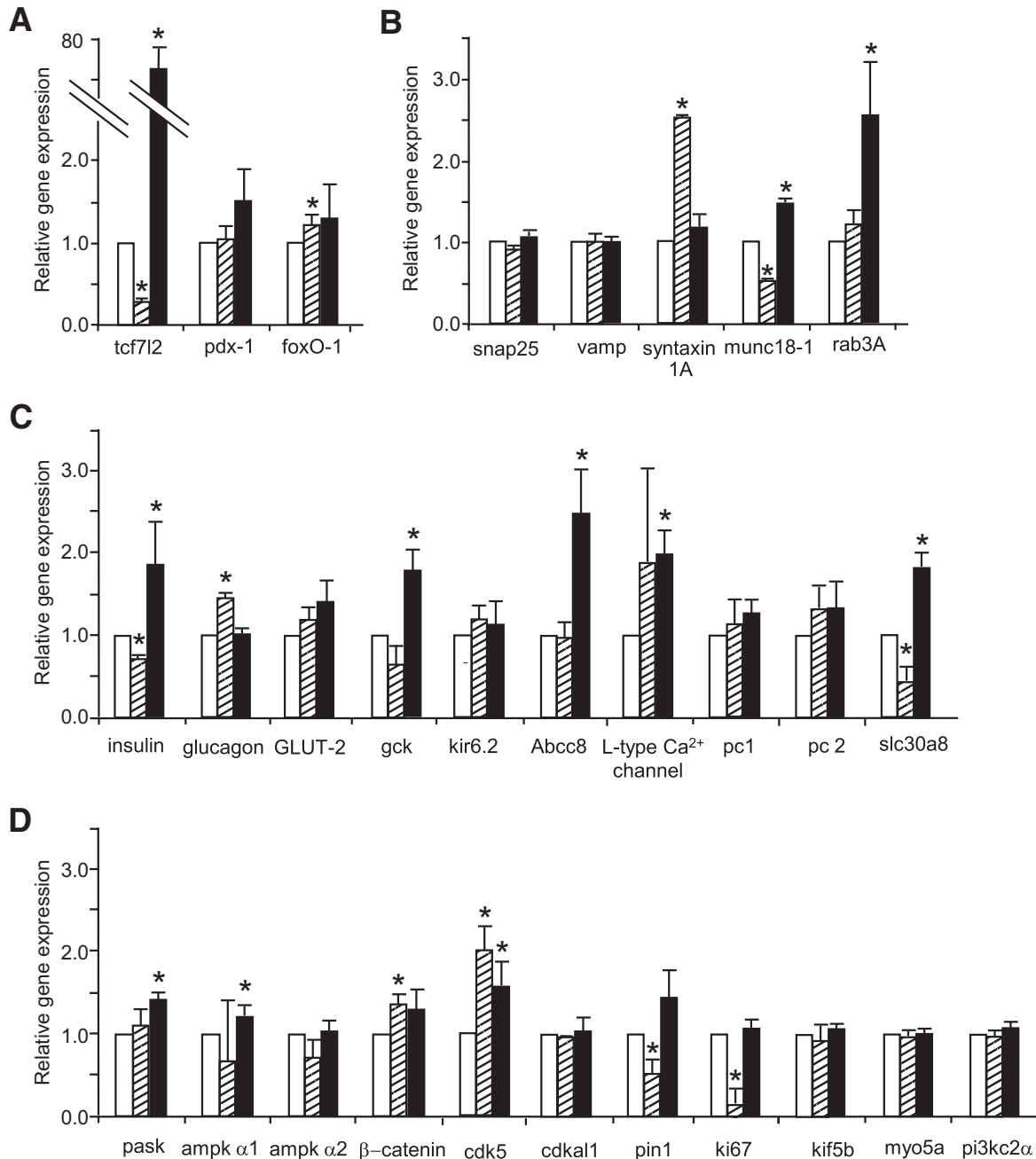


**FIG. 4.** Silencing and overexpression of TCF7L2 in mouse pancreatic islets lead to changes in expression of islet genes. Mouse pancreatic islets were cultured continuously in the presence of control (□), TCF7L2 siRNA (▨), or control and TCF7L2-EGFP (■) virus for 48 h. Total RNA was isolated as described in RESEARCH DESIGN AND METHODS, and islet gene expression was assessed by real-time PCR. Genes are grouped according to function: transcription factors (A), exocytosis (B), hormones, glucose sensing, and membrane transport (C), and signaling (D). Data are means  $\pm$  SEM,  $n = 3$ . \* $P < 0.05$  versus control.

C) in concurrence with studies in human islets (23). By contrast, insulin release stimulated by cell depolarization with high concentrations of  $K^+$  (30–50 mmol/l) was unaffected in islets (Fig. 1A) and INS-1(832/13) cells (Fig. 1C), implying a defect in metabolic signaling in response to elevated glucose (32) or a depletion of pool(s) of secretory granules with relatively high  $Ca^{2+}$  sensitivity (33). Whereas basal total cellular ATP and ADP levels were lower in TCF7L2-silenced mouse islets, glucose-induced changes in this ratio were augmented ( $0.46 \pm 0.10$ - and  $0.73 \pm 0.24$ -fold respectively compared with control; Fig. 2A). Similarly, glucose-induced changes in cytosolic-free calcium ion concentration ( $[Ca^{2+}]_i$ ; Fig. 2B and C) were

augmented in mouse islets (Fig. 2B and C). Glucose-induced changes in  $[Ca^{2+}]_i$  in INS-1(832/13) cells were not affected by TCF7L2 depletion (Fig. 2D), although the number of cells responding to elevated glucose was higher ( $46 \pm 10.3\%$  versus  $71 \pm 2.9\%$ ,  $P < 0.05$ ). In mouse islets, the stimulation of insulin secretion by GLP-1 at permissive (8 mmol/l) glucose concentrations was abolished when TCF7L2 was silenced (Fig. 1A).

**Impact of TCF7L2 overexpression on insulin secretion.** Given the reportedly higher levels of TCF7L2 mRNA in islets from carriers of the at-risk (T) allele (18), we examined the effect of overexpressing EGFP-tagged human TCF7L2 (TCF7L2-EGFP) in mouse islets or INS-1(832/

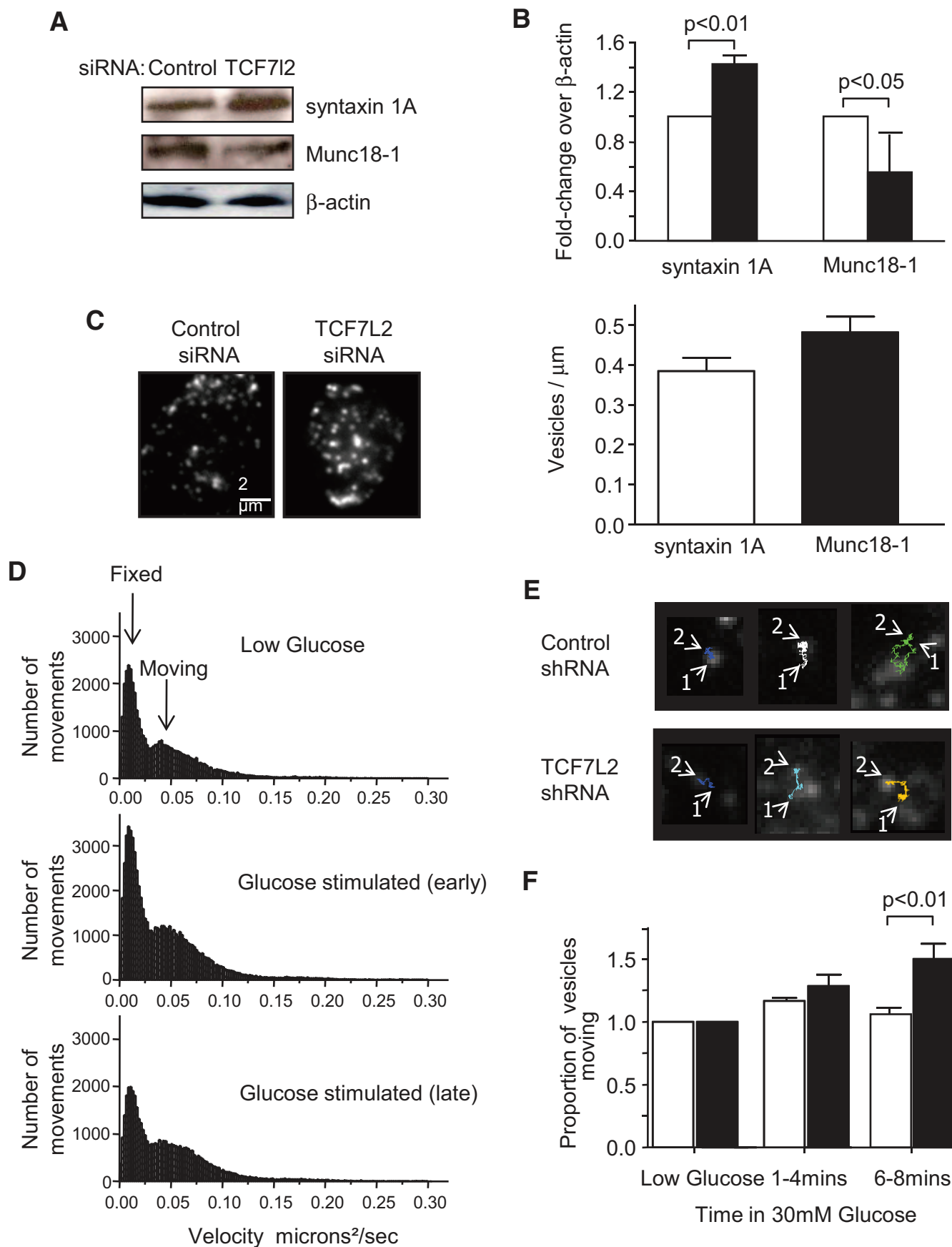


**FIG. 5.** Syntaxin 1A and Munc18-1 are regulated by TCF7L2. Mouse pancreatic islets were treated with TCF7L2 siRNA as described in RESEARCH DESIGN AND METHODS, and protein content was assessed by immunoblot analysis. **A:** Typical blots are shown. **B:** Quantification of immunoblots from three separate sets of samples using ImageJ is shown ( $\square$ , control siRNA;  $\blacksquare$ , TCF7L2 siRNA). TIRF microscopy of MIN6 cells treated with

13) cells. As expected, TCF7L2-EGFP was largely confined to the nucleoplasm (Fig. 3B). Increases in TCF7L2 protein level (approximately fourfold; Fig. 3A) in mouse islets did not affect glucose-stimulated (15 versus 3 mmol/l) insulin secretion (Fig. 3A). Likewise, overexpression of TCF7L2-EGFP did not affect glucose-induced  $[Ca^{2+}]_i$  increases in INS-1(832/13) cells (Fig. 3A and C). By contrast, the proportion of INS-1(832/13) cells responding to high glucose after transfection with TCF7L2-EGFP was lower ( $31.8 \pm 3.7\%$  versus  $47.5 \pm 4.0\%$ ,  $P < 0.05$ ) than in cells treated with control (EGFP-expressing) plasmid (Fig. 3D). The increase in  $[Ca^{2+}]_i$  in response to GLP-1 of cells overexpressing TCF7L2-EGFP was not different from that of EGFP-transfected cells (Fig. 3E).

**Impact of TCF7L2 expression levels on islet and  $\beta$ -cell gene expression.** To explore the mechanisms through which over- or underexpression of TCF7L2 may exert effects on insulin secretion, we examined the expression of genes that are involved in various aspects of  $\beta$ -cell function. Systematic real-time PCR analysis of scrambled or TCF7L2 siRNA-treated mouse islets was used to quantify the expression of 32 genes implicated in the control of  $\beta$ -cell function or survival (supplemental Table 1, available in an online appendix at <http://diabetes.diabetesjournals.org/cgi/content/full/db08-1187/DC1>, and Fig. 4). Of these, 25 displayed consistent changes in islets depleted of, or overexpressing, TCF7L2 (Fig. 4;  $n = 6$  separate mouse islet preparations). Depletion of TCF7L2 caused a small ( $\sim 20\%$ ) but significant decrease in preproinsulin mRNA levels, whereas overexpression of this factor approximately doubled preproinsulin mRNA levels. Conversely, preproglucagon mRNA was increased on TCF7L2 deletion, although overexpression of TCF7L2-EGFP exerted no clear effect on preproglucagon mRNA level. Neither TCF7L2 silencing nor overexpression exerted detectable effects on the mRNA level of the glucose transporter or on glucokinase, two key proteins involved in the control of glucose metabolism.

Islets treated with TCF7L2 siRNA also displayed decreased expression of preproinsulin but increased levels of mRNA encoding the TCF regulator  $\beta$ -catenin and the transcription factor FoxO-1, previously shown to influence the expression of pancreatic homeobox-1 (33). Similarly, mRNAs encoding the SNARE protein syntaxin 1A and the cell cyclin-dependent kinase cdk5 were increased by TCF7L2 silencing. In none of these cases did TCF7L2 overexpression cause a reciprocal decrease in mRNA levels. Expression of the *sec* family member Munc18-1 (34), the granule zinc transporter *ZnT8/Slc30a8* (35) (also recently associated with increased risk of type 2 diabetes [9]), the peptidylprolyl *cis/trans* isomerase pin1 (36), and the proliferation marker *ki67* (23) were all decreased when TCF7L2 was silenced. In the cases of Munc18-1 and *ZnT8*, TCF7L2 overexpression led to reciprocal increases in the coding mRNAs (Fig. 4), implicating the latter genes as direct transcriptional targets of TCF7L2. Changes in Munc18-1 and syntaxin 1A were also verified at the protein level by Western (immuno-) blotting (Fig. 5A and B). There was no change in the expression of the granule trafficking

proteins myosin5a and Kif5b or the signaling molecule PI3kinase-c2- $\alpha$ .

It was recently reported that patients carrying the SNP rs7903146 respond poorly to sulfonylurea treatment (37). We therefore determined the effect of TCF7L2 silencing on the expression of the ATP-sensitive  $K^+$  ( $K_{ATP}$ ) channel. Depleting TCF7L2 had no effect on the expression of either the Kir 6.2 or SUR1 components in mouse islets (Fig. 4).

**Effect of TCF7L2 on the subcellular distribution of secretory granules.** To explore the potential mechanisms through which changes in the expression of genes involved in granule dynamics and/or membrane fusion may affect secretion, we used TIRF microscopy of neuro-peptide-labeled dense core granules (38). This approach allowed the number of granules immediately beneath (100–200 nm) the plasma membrane to be determined in scrambled shRNA or anti-TCF7L2 shRNA-transfected MIN6 cells. No differences in granule number beneath the cell surface were observed ( $0.38 \pm 0.03$  and  $0.48 \pm 0.04$  granules/ $\mu m^{-2}$ ,  $P > 0.05$ , for 43 and 55 cells, respectively). There was an increase (41.8%,  $P < 0.01$ ) in the proportion of granules moving after 6 to 8 min of glucose stimulation, however, implying a defect in granule recruitment or tethering (Fig. 5D–F). To further explore this possibility, we used electron microscopy analysis of siRNA-transfected islets to quantify tethered granules. There was no significant difference in granule number per micron membrane between control and TCF7L2 siRNA-treated islets in either the morphologically docked pool ( $0.26 \pm 0.02$  versus  $0.19 \pm 0.02$ ,  $n = 15$ –17 cells; Fig. 6) or the pool within 200 nm of the plasma membrane ( $0.87 \pm 0.06$  versus  $0.78 \pm 0.05$ ,  $n = 15$ –17 cells).

**Effect of TCF7L2 on granule fusion and  $Ca^{2+}$  currents.** These results implicated defects in the machinery of vesicle fusion in cells depleted of TCF7L2. We hypothesized that the differences may be observed in response to “mild” stimulation with glucose, resulting in oscillatory  $[Ca^{2+}]_i$  increases, but may be lost when  $[Ca^{2+}]_i$  is raised for a lengthy period during  $K^+$  depolarization (see Fig. 1A). To test this hypothesis, the effect of TCF7L2 silencing on granule fusion was measured using a whole-cell patch-clamp. Stimulation protocols were used to provide oscillatory increases in  $[Ca^{2+}]_i$  as observed during stimulation with glucose. Exocytosis was triggered by trains of membrane depolarizations of different duration:  $20 \times 0.25$  s,  $10 \times 0.50$  s, or  $10 \times 2.5$  s. The depolarizations elicited similar exocytotic responses from the TCF7L2-depleted and control cells with fusion dynamics strongly depending on the stimulation duration (Fig. 7) and  $Ca^{2+}$  current being essentially identical in the two groups. The initial cell capacitance of the TCF7L2-depleted cells was slightly higher than that of control ( $11.4 \pm 0.7$  pF versus  $8.94 \pm 0.5$  pF,  $P < 0.05$ ) and the exocytotic response to the membrane depolarization was significantly reduced in the TCF7L2-depleted cells as compared with the control (Fig. 7A) for all pulse durations with the extent of the inhibition decreasing from  $\sim 80\%$  (0.2 s) to  $\sim 40\%$  (2.5 s).

TCF7L2 shRNA and quantification of granule number at the cell surface was as described in RESEARCH DESIGN AND METHODS. Images shown are averages of 1-s movies acquired at 50 Hz and 20-ms exposure at 100 nm/pixel. Data are means  $\pm$  SEM,  $n = 3$  (30–35 cells per condition) (C). Scale bar = 2  $\mu m$ . Example graphs (D) of granule movement analysis from a representative control cell at different times and representative tracks (E) of the different categories of granule movement observed after the addition of 30 mmol/l glucose. All tracks are 30 s or longer (1 = beginning of track, 2 = end), and comparison (F) of the proportion of moving granules in TCF7L2 silenced and control  $\beta$ -cells before and during application of high glucose ( $n = 5$ ; 15–25 separate cells per condition;  $\square$ , scrambled;  $\blacksquare$ , TCF7L2 shRNA). (A high-quality digital representation of this figure is available in the online issue.)

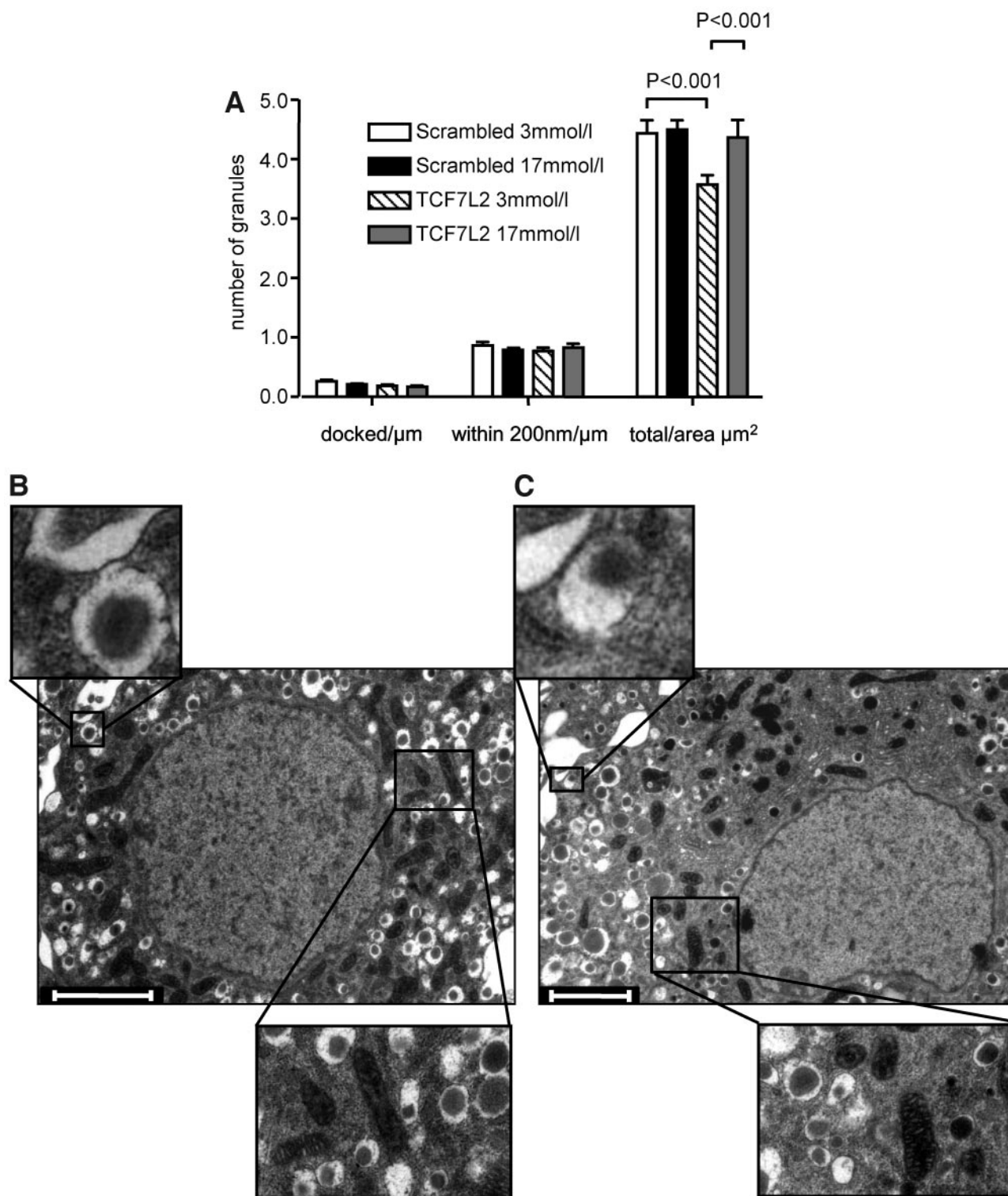


**FIG. 6.** TCF7L2 expression does not affect the morphologically docked granule pool. **A:** Mouse islets were transfected with siRNA as described. The total number of granules, morphologically docked, and within 200 nm of the membrane pools were analyzed as described in RESEARCH DESIGN AND METHODS;  $n = 14$ – $16$  cells per condition. **B** and **C:** Representative  $\beta$ -cells with examples of docked granules and mitochondria (scrambled siRNA [**B**] and TCF7L2 siRNA [**C**]). Scale bars = 2  $\mu\text{m}$ .

## DISCUSSION

The principal aims of this study were to determine the impact of altering the level of expression of TCF7L2 on glucose sensing and insulin secretion in pancreatic  $\beta$ -cells and to explore the underlying molecular mechanisms. In addition to describing changes in the expres-

sion of genes involved in  $\beta$ -cell survival and proliferation (pin1, Ki67, and so on) consistent with earlier findings (23,37), we demonstrate that several genes involved in  $\beta$ -cell function, that is, hormone production and secretion, are also under the control of TCF7L2.

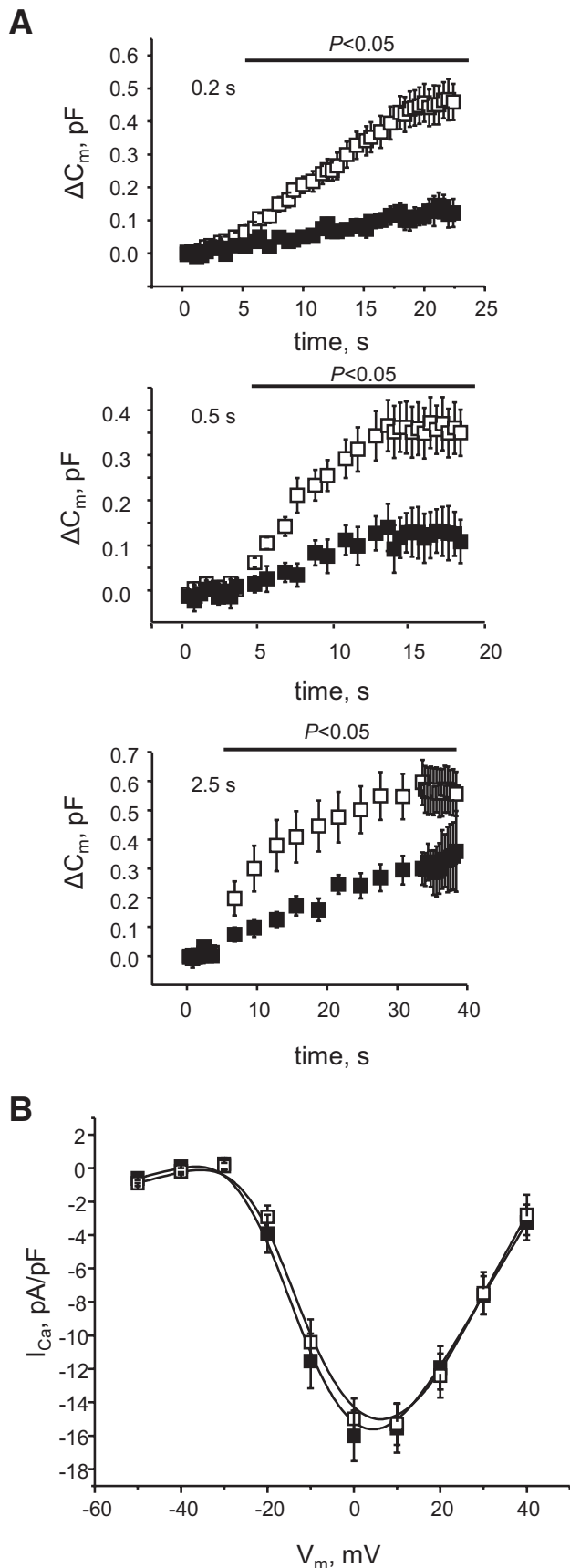


**FIG. 7.** TCF7L2 depletion affects membrane capacitance or voltage-gated  $Ca^{2+}$  currents. Changes in  $\beta$ -cell membrane capacitance ( $C_m$ ) in response to a train of 10 pulses of 200-, 500-, or 2,500-msec depolarizations from  $-70$  mV to 0 mV ( $n = 16$ , scrambled;  $n = 18$ , TCF7L2). **A:**

**TCF7L2 regulation of genes involved in insulin maturation.** It has previously been suggested that TCF7L2 may regulate the promoters for prohormone convertase-1 and -2 (17) and hence exert an effect on proinsulin processing. The expression of neither gene was altered by manipulating TCF7L2 levels in mouse islets (Fig. 4). Mouse islets overexpressing TCF7L2 displayed higher *slc30a8* (another gene associated with type 2 diabetes, which plays a role in insulin processing) (9,39) gene expression (Fig. 4), whereas mouse islets in which TCF7L2 had been silenced displayed decreased *slc30a8* mRNA levels. However, although preproinsulin gene expression was reduced (Fig. 4), no differences in granule number (Fig. 6), insulin content, or insulin processing (supplemental Fig. 1, available in the online appendix) were observed after treatment with TCF7L2 siRNA, suggesting that the acute effects of TCF7L2 depletion on insulin secretion are not the result of changes in insulin production.

**TCF7L2 regulation of  $\beta$ -cell survival.** TCF7L2 knock-down reduced expression of pin1 and ki67, a marker of  $\beta$ -cell proliferation (23). However, electron microscopy analysis of  $\beta$ -cells revealed no apparent change in cellular ultrastructure indicative of endoplasmic reticulum stress, mitochondrial damage, or nuclear condensation. The observed inhibition of glucose-mediated insulin secretion seems unlikely to be the result of decreased cell viability.

**Control by TCF7L2 of insulin synthesis and release.** The present study shows that reducing TCF7L2 expression in the short term (48 h) affects the normal function of the  $\beta$ -cell, leading to a decrease in glucose-stimulated insulin secretion (Fig. 1A–C). These changes were not associated with major perturbations in the expression of genes encoding the glucose transporter GLUT2 or glucokinase (Fig. 4). Correspondingly, glucose-stimulated increases in cytosolic-free  $[Ca^{2+}]$  and cellular adenine nucleotide concentration (Fig. 2) were slightly enhanced on TCF7L2 depletion and no changes in the content of  $\beta$ -cell calcium channel subunits, sodium/calcium exchangers, PMCA, or the calcium sensing synaptotagmins were observed (supplemental Table 1, available in the online appendix). Voltage-gated  $Ca^{2+}$  currents were unaltered (Fig. 7B), showing that the channel capacity was unaffected.

These observations led us to postulate that the secretory deficiency may be the result of defects at a late step in the exocytotic process. Consistent with this view, real-time PCR and immunoblot analysis of mouse islets treated with TCF7L2 siRNA revealed increases in syntaxin 1A but decreases in Munc18-1, mRNA, and protein levels (Figs. 4 and 5A–B). Fourfold overexpression of TCF7L2 increased Munc18-1 and rab3a mRNA levels but did not alter syntaxin 1A expression or insulin secretion in islets, suggesting syntaxin as the important effector of TCF7L2 effects. It has been suggested that TCF7L2 can act as a transcriptional repressor (40). Our overexpression data do not suggest such a function for this clone.

**Absolute change in membrane capacitance.** The number of data points shown is reduced compared with those acquired by  $200\times$  for clarity. To filter the data, a threshold for capacitance (7 pF bottom, 13 pF top) was set considering the smaller/larger cells outliers. The pipette solution contained (mmol/l): 125 Cs-glutamate, 10 NaCl, 10 CsCl, 1 MgCl<sub>2</sub>, 3 MgATP, 0.1 cAMP, 5 HEPES (pH 7.15 with CsOH). The extracellular (bath) solution contained (mmol/l): 118 NaCl, 20 TEA-Cl, 5.6 KCl, 5 glucose, 2.6 CaCl<sub>2</sub>, 1.2 MgCl<sub>2</sub>, 5 HEPES (pH 7.4 with NaOH). **B:** Voltage-gated  $Ca^{2+}$  currents ( $n = 22$ , scrambled;  $n = 27$ , TCF7L2). ■, TCF7L2 siRNA; □, scrambled siRNA.

Increased levels of syntaxin 1A can perturb insulin secretion. Transgenic mice overexpressing syntaxin 1A exhibit insulin secretory defects and reduced  $\text{Ca}^{2+}$  currents (41). We did not observe evidence for any corresponding changes in free  $[\text{Ca}^{2+}]_i$  in mouse islets treated with siRNA for TCF7L2 (Fig. 2A), suggesting that the influence of augmented syntaxin 1A expression on insulin release events is likely to be exerted through an alteration on the fusion potential of the granules in response to a glucose challenge.

Munc18-1 is an important modulator of the folded conformation of syntaxin 1A, and decreased Munc18-1 expression has been seen in islets from patients with type 2 diabetes (42) and GK rats (43). In PC12 cells, increased syntaxin 1A and decreased Munc18-1 levels had a negative effect on membrane trafficking and catecholamine secretion (44). TCF7L2 consensus binding sites (WWCAAAG) were identified in the 5' untranslated region of both the human and mouse syntaxin 1A and Munc18-1 (using TFExplorer [http://tfexplorer.org]), suggesting that they may be direct targets for regulation by TCF7L2 (supplemental Fig. 2, available in the online appendix). The increase in syntaxin 1A and decrease in Munc18-1 levels described here may account, at least in part, for the defective glucose-stimulated insulin secretion observed in TCF7L2-depleted cells.

Despite a strong reduction in insulin secretion, we did not observe any clear alteration in the number of near-plasma membrane granules in TCF7L2 siRNA-treated islets by TIRF (Fig. 5C) or electron microscopy (Fig. 6A). There were no observable alterations in the expression of trafficking proteins Myosin5a or Kif5b (Fig. 4) or in the actin network structure (supplemental Fig. 4, available in the online appendix), suggesting that granule targeting to the cell surface is unaffected. Under conditions in which a repeated mild stimulation was applied (Fig. 7B) to mimic the effects of glucose on  $[\text{Ca}^{2+}]_i$ ,  $\beta$ -cells silenced for TCF7L2 showed impaired capacitance increases. The inhibitory effects of TCF7L2 deletion were substantially more marked at shorter pulse durations (0.2 s), most closely mimicking the spontaneous action potentials normally triggering insulin exocytosis in response to glucose than at longer pulse durations (0.5 or 2.5 s), approaching the effects of sustained depolarization with KCl (Fig. 7A). Coupled with the increase in granule movements seen in the later stages of glucose stimulation by TIRF microscopy (Fig. 5E and F), this observation suggests that the selective inhibition of glucose- but not KCl-stimulated insulin secretion may reflect the combined effect of failure to recruit competent granules and defective vesicle fusion during repetitive  $[\text{Ca}^{2+}]_i$  increases.

The present studies demonstrate that near complete ablation of TCF7L2 is likely to have marked effects on insulin release from pancreatic  $\beta$ -cells. It should be emphasized, however, that the extent of these changes is likely to considerably exceed those observed in carriers of the at-risk T-allele of TCF7L2. Future studies will be required to assess how more subtle variations in TCF7L2 level impact on  $\beta$ -cell function and survival.

In conclusion, lack of functional TCF7L2 leads to defective glucose-stimulated insulin secretion. This is probably attributable, in part, to changes in the expression of key regulatory genes and processes involved in granule recruitment and exocytosis.

## ACKNOWLEDGMENTS

This study was funded by grants to G.A.R. from the Wellcome Trust (program grants 067081/Z/02/Z and 081958/Z/07/Z), MRC (G0401641), National Institutes of Health (ROI DKO71962-01), and European Union FP6 (Savebeta) and to G.S.X. from the Juvenile Diabetes Research Foundation (JDRF 3-2005-112) and European Foundation for the Study of Diabetes (EFSD Albert Renold Travel Fellowship).

No potential conflicts of interest relevant to this article were reported.

We thank Prof. Andrew Halestrap and Nigel Edgell (University of Bristol) for their advice on total ADP measurements; Nasret Harun, Saharnaz Vakhshouri, and Gao Sun for excellent technical assistance; and Dr. C. Newgard (Duke University) for providing INS-1(832/13) cells. We thank Dr. Lorna Harris and Jonathan Locke for useful discussions.

## REFERENCES

- Zimmet P, Alberti KG, Shaw J: Global and societal implications of the diabetes epidemic. *Nature* 414:782–787, 2001
- Rutter GA, Parton LE: The beta-cell in type 2 diabetes and in obesity. *Front Horm Res* 36:118–134, 2008
- Busch CP, Hegele RA: Genetic determinants of type 2 diabetes mellitus. *Clin Genet* 60:243–254, 2001
- Baier LJ, Permana PA, Yang X, Pratley RE, Hanson RL, Shen GQ, Mott D, Knowler WC, Cox NJ, Horikawa Y, Oda N, Bell GI, Bogardus C: A calpain-10 gene polymorphism is associated with reduced muscle mRNA levels and insulin resistance. *J Clin Invest* 106:R69–R73, 2000
- Hattersley AT, Turner RC, Permutt MA, Patel P, Tanizawa Y, Chiu KC, O'Rahilly S, Watkins PJ, Wainscoat JS: Linkage of type 2 diabetes to the glucokinase gene. *Lancet* 339:1307–1310, 1992
- Stoffel M, Patel P, Lo YM, Hattersley AT, Lucassen AM, Page R, Bell GI, Bell GI, Turner RC, Wainscoat JS: Missense glucokinase mutation in maturity-onset diabetes of the young and mutation screening in late-onset diabetes. *Nat Genet* 2:153–156, 1992
- Frayling TM: Genome-wide association studies provide new insights into type 2 diabetes aetiology. *Nat Rev Genet* 8:657–662, 2007
- Saxena R, Voight BF, Lyssenko V, Burt NP, de Bakker PI, Chen H, Roix JJ, Kathiresan S, Hirschhorn JN, Daly MJ, Hughes TE, Groop L, Althuler D, Almgren P, Florez JC, Meyer J, Ardlie K, Bengtsson BK, Isomaa B, Lettre G, Lindblad U, Lyon HN, Melander O, Newton-Cheh C, Nilsson P, Orholm-Melander M, Rastam L, Speliotes EK, Taskiran MR, Tuomi T, Guiducci C, Berglund A, Carlson J, Gianniny L, Hackett R, Hall L, Holmkvist J, Laurila E, Sjogren M, Sterner M, Surti A, Svensson M, Svensson M, Tewhey R, Blumenshtiel B, Parkin M, Defelice M, Barry R, Brodeur W, Camarata J, Chia N, Fava M, Gibbons J, Handsaker B, Healy C, Nguyen K, Gates C, Sougnez C, Gage D, Nizzari M, Gabriel SB, Chim GW, Ma Q, Parikh H, Richardson D, Riecke D, Purcell S: Genome-wide association analysis identifies loci for type 2 diabetes and triglyceride levels. *Science* 316:1331–1336, 2007
- Sladek R, Rocheleau G, Rung J, Dina C, Shen L, Serre D, Boutin P, Vincent D, Belisle A, Hadjadj S, Balkau B, Heude B, Charpentier G, Hudson TJ, Montpetit A, Pshezhetsky AV, Prentki M, Posner BI, Balding DJ, Meyre D, Polychronakos C, Froguel P: A genome-wide association study identifies novel risk loci for type 2 diabetes. *Nature* 445:881–885, 2007
- Zeggini E, Weedon MN, Lindgren CM, Frayling TM, Elliott KS, Lango H, Timpson NJ, Perry JR, Rayner NW, Freathy RM, Barrett JC, Shields B, Morris AP, Ellard S, Groves CJ, Harries LW, Marchini JL, Owen KR, Knight B, Cardon LR, Walker M, Hitman GA, Morris AD, Doney AS, McCarthy MI, Hattersley AT: Replication of genome-wide association signals in UK samples reveals risk loci for type 2 diabetes. *Science* 316:1336–1341, 2007
- Grant SF, Thorleifsson G, Reynisdottir I, Benediktsson R, Manolescu A, Sainz J, Helgason A, Stefansson H, Emilsson V, Helgadóttir A, Styrkarsdóttir U, Magnusson KP, Walters GB, Palsdóttir E, Jonsdóttir T, Gudmundsdóttir T, Gylfason A, Saemundsdóttir J, Wilensky RL, Reilly MP, Rader DJ, Bagger Y, Christiansen C, Gudnason V, Sigurdsson G, Thorsteinsdóttir U, Gulcher JR, Kong A, Stefansson K: Variant of transcription factor 7-like 2 (TCF7L2) gene confers risk of type 2 diabetes. *Nat Genet* 38:320–323, 2006
- Groves CJ, Zeggini E, Minton J, Frayling TM, Weedon MN, Rayner NW, Hitman GA, Walker M, Wiltshire S, Hattersley AT, McCarthy MI: Association analysis of 6736 UK subjects provides replication and confirms

- TCF7L2 as a type 2 diabetes susceptibility gene with a substantial effect on individual risk. *Diabetes* 55:2640–2644, 2006
13. Zhang C, Qi L, Hunter DJ, Meigs JB, Manson JE, van Dam RM, Hu FB: Variant of transcription factor 7-like 2 (TCF7L2) gene and the risk of type 2 diabetes in large cohorts of US women and men. *Diabetes* 55:2645–2648, 2006
  14. Zeggini E, McCarthy MI: TCF7L2: the biggest story in diabetes genetics since HLA? *Diabetologia* 50:1–4, 2007
  15. Moon RT, Kohn AD, De Ferrari GV, Kaykas A: WNT and beta-catenin signalling: diseases and therapies. *Nat Rev Genet* 5:691–701, 2004
  16. Slattey ML, Folsom AR, Wolff R, Herrick J, Caan BJ, Potter JD: Transcription factor 7-like 2 polymorphism and colon cancer. *Cancer Epidemiol Biomarkers Prev* 17:978–982, 2008
  17. Loos RJ, Franks PW, Francis RW, Barroso I, Gribble FM, Savage DB, Ong KK, O'Rahilly S, Wareham NJ: TCF7L2 polymorphisms modulate proinsulin levels and beta-cell function in a British European population. *Diabetes* 56:1943–1947, 2007
  18. Lyssenko V, Lupi R, Marchetti P, Del GS, Orho-Melander M, Almgren P, Sjogren M, Ling C, Eriksson KF, Lethagen AL, Mancarella R, Berglund G, Tuomi T, Nilsson P, Del PS, Groop L: Mechanisms by which common variants in the TCF7L2 gene increase risk of type 2 diabetes. *J Clin Invest* 117:2155–2163, 2007
  19. Elbein SC, Chu WS, Das SK, Yao-Borengasser A, Hasstedt SJ, Wang H, Rasouli N, Kern PA: Transcription factor 7-like 2 polymorphisms and type 2 diabetes, glucose homeostasis traits and gene expression in US participants of European and African descent. *Diabetologia* 50:1621–1630, 2007
  20. Cauchi S, Meyre D, Dina C, Choquet H, Samson C, Gallina S, Balkau B, Charpentier G, Pattou F, Stetsyuk V, Scharfmann R, Staels B, Fruhbeck G, Froguel P: Transcription factor TCF7L2 genetic study in the French population: expression in human beta-cells and adipose tissue and strong association with type 2 diabetes. *Diabetes* 55:2903–2908, 2006
  21. Wang J, Kuusisto J, Vanttinen M, Kuulasmaa T, Lindstrom J, Tuomilehto J, Uusitupa M, Laakso M: Variants of transcription factor 7-like 2 (TCF7L2) gene predict conversion to type 2 diabetes in the Finnish Diabetes Prevention Study and are associated with impaired glucose regulation and impaired insulin secretion. *Diabetologia* 50:1192–1200, 2007
  22. Korinek V, Barker N, Moerer P, van DE, Huls G, Peters PJ, Clevers H: Depletion of epithelial stem-cell compartments in the small intestine of mice lacking Tcf-4. *Nat Genet* 19:379–383, 1998
  23. Shu L, Sauter NS, Schulthess FT, Matveyenko AV, Oberholzer J, Maedler K: TCF7L2 regulates cell survival and function in human pancreatic islets. *Diabetes* 57:645–653, 2008
  24. Miyazaki J, Araki K, Yamato E, Ikegami H, Asano T, Shibasaki Y, Oka Y, Yamamura K: Establishment of a pancreatic beta cell line that retains glucose-inducible insulin secretion: special reference to expression of glucose transporter isoforms. *Endocrinology* 127:126–132, 1990
  25. Hohmeier HE, Mulder H, Chen G, Henkel-Rieger R, Prentki M, Newgard CB: Isolation of INS-1-derived cell lines with robust ATP-sensitive K<sup>+</sup> channel-dependent and -independent glucose-stimulated insulin secretion. *Diabetes* 49:424–430, 2000
  26. Rutter MA, Rutter GA: Glucose or insulin, but not zinc ions, inhibit glucagon secretion from mouse pancreatic alpha-cells. *Diabetes* 54:1789–1797, 2005
  27. Ainscow EK, Zhao C, Rutter GA: Acute overexpression of lactate dehydrogenase-A perturbs beta-cell mitochondrial metabolism and insulin secretion. *Diabetes* 49:1149–1155, 2000
  28. Robb-Gaspers LD, Burnett P, Rutter GA, Denton RM, Rizzuto R, Thomas AP: Integrating cytosolic calcium signals into mitochondrial metabolic responses. *EMBO J* 17:4987–5000, 1998
  29. Nilsson T, Schultz V, Berggren PO, Corkey BE, Tornheim K: Temporal patterns of changes in ATP/ADP ratio, glucose 6-phosphate and cytoplasmic free Ca<sup>2+</sup> in glucose-stimulated pancreatic beta-cells. *Biochem J* 314:91–94, 1996
  30. Olofsson C, Göpel S, Barg S, Galvanovskis J, Ma X, Salehi A, Rorsman P, Eliasson L: Fast insulin secretion reflects exocytosis of docked granules in mouse pancreatic B-cells. *Pflugers Arch* 444:43–51, 2002
  31. Kanno T, Ma X, Barg S, Eliasson L, Galvanovskis J, Göpel S, Larsson M, Renström E, Rorsman P: Large dense-core vesicle exocytosis in pancreatic [beta]-cells monitored by capacitance measurements. *Methods* 33:302–311, 2004
  32. Rutter GA, Tsuboi T, Ravier MA: Ca<sup>2+</sup> microdomains and the control of insulin secretion. *Cell Calcium* 40:539–551, 2006
  33. Wan QF, Dong Y, Yang H, Lou X, Ding J, Xu T: Protein kinase activation increases insulin secretion by sensitizing the secretory machinery to Ca<sup>2+</sup>. *J Gen Physiol* 124:653–662, 2004
  34. Khvotchev M, Dulubova I, Sun J, Dai H, Rizo J, Sudhof TC: Dual modes of Munc18-1/SNARE interactions are coupled by functionally critical binding to syntaxin-1 N terminus. *J Neurosci* 27:12147–12155, 2007
  35. Chimienti F, Devergnas S, Pattou F, Schuit F, Garcia-Cuenca R, Vandewalle B, Kerr-Conte J, Van LL, Grunwald D, Favier A, Seve M: In vivo expression and functional characterization of the zinc transporter ZnT8 in glucose-induced insulin secretion. *J Cell Sci* 119:4199–4206, 2006
  36. Chen SY, Wulf G, Zhou XZ, Rubin MA, Lu KP, Balk SP: Activation of beta-catenin signaling in prostate cancer by peptidyl-prolyl isomerase Pin1-mediated abrogation of the androgen receptor-beta-catenin interaction. *Mol Cell Biol* 26:929–939, 2006
  37. Pearson ER, Donnelly LA, Kimber C, Whitley A, Doney AS, McCarthy MI, Hattersley AT, Morris AD, Palmer CN: Variation in TCF7L2 influences therapeutic response to sulfonylureas: a GoDARTs study. *Diabetes* 56:2178–2182, 2007
  38. Tsuboi T, McMahon HT, Rutter GA: Mechanisms of dense core vesicle recapture following 'kiss and run' ('cavicapture') exocytosis in insulin-secreting cells. *J Biol Chem* 279:47115–47124, 2004
  39. Kirchhoff K, Machicao F, Haupt A, Schafer SA, Tschritter O, Staiger H, Stefan N, Haring HU, Fritsche A: Polymorphisms in the TCF7L2, CDKAL1 and SLC30A8 genes are associated with impaired proinsulin conversion. *Diabetologia* 51:597–601, 2008
  40. Tang W, Dodge M, Gundapaneni D, Michnoff C, Roth M, Lum L: A genome-wide RNAi screen for Wnt/+ -catenin pathway components identifies unexpected roles for TCF transcription factors in cancer. *Proc Natl Acad Sci* 105:9697–9702, 2008
  41. Lam PP, Leung YM, Sheu L, Ellis J, Tsushima RG, Osborne LR, Gaisano HY: Transgenic mouse overexpressing syntaxin-1A as a diabetes model. *Diabetes* 54:2744–2754, 2005
  42. Ostenson CG, Gaisano H, Sheu L, Tibell A, Bartfai T: Impaired gene and protein expression of exocytotic soluble N-ethylmaleimide attachment protein receptor complex proteins in pancreatic islets of type 2 diabetic patients. *Diabetes* 55:435–440, 2006
  43. Zhang W, Khan A, Ostenson CG, Berggren PO, Efendic S, Meister B: Down-regulated expression of exocytotic proteins in pancreatic islets of diabetic GK rats. *Biochem Biophys Res Commun* 291:1038–1044, 2002
  44. Rowe J, Corradi N, Malosio ML, Taverna E, Halban P, Meldolesi J, Rosa P: Blockade of membrane transport and disassembly of the Golgi complex by expression of syntaxin 1A in neurosecretion-incompetent cells: prevention by rbSEC1. *J Cell Sci* 112:1865–1877, 1999